

Fibre Distribution and Dosage Performance on the Impact Resistance of Oil Palm Shells Concrete with Hybrid Polypropylene Fibre-Mesh

Zakaria Che Muda^{1,*}, Mohamed Hafez¹, Agusril Syamsir², Erni Syawani Zahari², Md. Ashrafal Alam³, and As'ad Zakaria⁴

¹Faculty of Engineering and Quantity Surveying, INTI-International University, Persiaran Perdana BBN Putra Nilai, 71800 Nilai, Malaysia

²Institute of Energy Infrastructure, Universiti Tenaga Nasional, Putrajaya Campus, Jalan IKRAM-UNITEN, 43000, Kajang, Selangor, Malaysia

³Department of Civil Engineering, University of Asia Pacific, Level-6, 74/A, Green Road, Farmgate, Dhaka-1215, Bangladesh

⁴Institute of Energy Systems, School of Engineering, University of Edinburgh, Edinburgh EH9 3FB, UK

Received: 10 May 2024, Revised: 29 Jun. 2024, Accepted: 10 Jul. 2024.

Published online: 1 Nov. 2024.

Abstract: This research paper investigates the effect of top and bottom fibre distribution configurations against 1%, 2%, and 3% fibre volume fractions on the impact performance of lightweight oil palm shells concrete slabs with polypropylene fibres and polypropylene mesh under low-velocity impact projectile. Lightweight aggregate in concrete utilizing agricultural waste recycling materials has been used to produce a green product for the construction industry to prevent environmental pollution. Slabs of dimensions 300mm x 300mm and 40mm thickness are subjected to a drop-weight impact test using a self-fabricated rig and a 1.05 kg steel ball dropped from a height of 0.57 m. The study's main objectives are to analyze the relationship between impact energy and crack resistance against fibre volume fractions for top and bottom fibre distribution. The results indicate that the bottom fibre distribution outperforms the top fibre distribution in all the impact-related factors. An increase in PP fibre dosage leads to significant improvements in the impact behaviour of the slabs. Bi-linear equations were proposed for top and bottom fibre distribution between service and ultimate impact behaviour against fibre volume fraction. The top fibre distribution has more segmental failure zones than the bottom fibre; however, the bottom fibre distribution has better impact performance and post-cracking ductility. PP fibres control the micro-cracks at the initial phase, while the PP mesh bridges the minor cracks at the failure phase.

Keywords: waste recycling, green product, environmental pollution, impact behaviour, impact energy, crack resistance, oil palm shell aggregate, polypropylene fibres, polypropylene mesh.

1 Introduction

The construction industry's search for sustainable and eco-friendly green products has reached a critical stage in preventing environmental pollution [1]. Agricultural waste recycling of aggregates derived from agricultural by-products and residues can be used as a replacement for traditional aggregates in concrete [2, 3, 4, 5]. Farahani et al. [6] investigated the feasible use of high-volume agriculture and industrial waste in producing environmentally sustainable lightweight aggregate concrete. The utilization of waste materials that can act as a sensible substitute for natural aggregates or cement for concrete. It offers a mitigating measure against the adverse environmental effects associated with the concrete industry [7].

Palm kernel shells are by-products of the palm oil industry. They can be used as structural lightweight aggregates in concrete with good mechanical strength, low-density concrete, and thermal insulation properties. These materials

offer a sustainable and eco-friendly solution for reducing the environmental impact of concrete production. It is also crucial to study the impact strength characteristics and evaluate the performance of these materials for use in the building industry. Kareem et al. [8] mentioned in their review paper that utilizing oil palm shell (OPS) as an alternative aggregate was both effective and environmentally sustainable. This conclusion was drawn from the positive outcomes of the prior studies with diverse methods, procedures, and materials employed to establish the optimum OPS content that significantly improved the fresh and mechanical properties of lightweight aggregate concrete.

Aslam et al. [9] achieved their objectives of researching to produce structural lightweight aggregate concrete using oil palm shells and oil palm boiler clinkers as coarse lightweight aggregates with adequate mechanical strength.

Abdul Rahman et al. [10] investigated the efficacy of substituting 80% of conventional weight aggregate in

*Corresponding author e-mail: zakaria.chemuda@newinti.edu.my

concrete with lightweight oil palm shell (OPS) aggregate. This replacement resulted in a 16% reduction in density compared to regular concrete. However, the study found a decrease of 35% in compressive strength compared to the compressive strength of 30 MPa for normal-weight concrete.

Recent research has indicated that achieving higher strength grades in structural OPS concrete is possible. Mannan *et al.* [11] achieved a compressive strength of 32.84 N/mm² for OPS concrete using 20% polyvinyl alcohol. Mo *et al.* [12] found that the 28-day compressive strength of ranges with and without fibres was between 37 and 49.4 MPa. Maghfouri *et al.* [13] observed a compressive strength of 40.5 N/mm² with 100% OPS aggregate replacement. Aslam *et al.* [14] discovered that incorporating 50% oil palm boiler clinker in OPS concrete resulted in a compressive strength of 53.3 N/mm².

Yap *et al.* [15] studied the impact of using steel fibres at a dosage ranging from 0.25% to 1.00% in oil palm shell concrete (OPSC). They concluded that adding 1% steel fibres yielded the highest flexural strength of 8.2 MPa and compressive strength of 47 MPa.

The incorporation of fibres into lightweight concrete has been demonstrated to enhance various engineering properties. These improvements encompass flexural strength, thermal shock resistance, fracture toughness, impact resistance, and fatigue load-bearing capabilities [16]. In a study conducted by Hwang *et al.* [17], it was emphasized that impact resistance signifies a material's capacity to absorb energy, making it a desirable attribute in fibre-reinforced composites. Furthermore, Cifuentes *et al.* [18] noted that in cementitious materials, the typical application of fibre reinforcement aims to augment toughness and energy absorption capacity while concurrently diminishing micro cracking within the material matrix. Aliabdo *et al.* [19] suggested that various factors, such as the type and quantity of fibres, shape of steel fibres, type of coarse aggregate, and water-to-cement ratio, influence the impact resistance of concrete. Saidani *et al.* [20] emphasized that several factors, such as the aspect ratio, fibre length, volume fraction, and tensile strength of the fibres, play a pivotal role in optimizing the efficiency of fibres in concrete.

Furthermore, Bagherzadeh *et al.* [21] conducted a study that showed incorporating nylon and polypropylene fibres enhances the properties of concrete, with notable improvements in tensile strength, first crack strength, and resistance to impact. Islam and Bindiganavile attributed the increase in energy dissipation in concrete under impact loading to the presence of short, discrete polymeric fibres [22]. Mastali and Dalvand [23] investigated that reinforced lightweight concrete structures with higher fibre content and longer fibre lengths exhibit increased impact resistance. This improvement is attributed to the planar orientation's effectiveness and the fibbers' bridging action. Li *et al.* [24]

experimented with a mortar and concrete reinforced with various lengths of chopped carbon fibres. They aimed to enhance impact resistance and resistance to shockwaves of the fibre-reinforced mortar and concrete. Nia *et al.* [25] observed increased impact resistance was more significant with increased fibres. Their findings indicated that hooked-ends steel fibres were more effective in improving impact resistance due to higher tensile strength, better bond, and anchorage when compared to polypropylene fibres.

Yew *et al.* [26] investigated oil palm shell concrete reinforced with monofilament-polypropylene (PP) twisted bundles with different lengths. They found that the fibres with a larger length have the best mechanical strength. Kim *et al.* [27] studied the impact resistance of hybrid fibre-reinforced concrete made with oil palm shell aggregates. It evaluates the influence of different types and combinations of fibres on the impact strength of the concrete. Islam *et al.* [28] researched OPS concrete, revealing that adding 0.5% steel fibres substantially increased the first crack load by 1.5 to 3.5 times compared with the control without fibre. Furthermore, the ultimate impact energy for a mix with uncrushed OPS aggregate is 15-152% higher than crushed OPS aggregate.

Zamzani *et al.* [29] experimented on lightweight foamed concrete with coconut coir and found enhanced mechanical properties. Adding the coconut coir fibres improved the post-peak behaviour of load-deflection curves and enhanced their mechanical strength. Mohamad *et al.* [30] researched adding banana skin powder and palm oil fuel ash in lightweight foamed concrete. Their study showed that increasing the percentage of banana skin powder and palm oil fuel ash enhanced the mechanical properties of lightweight foamed concrete; however, increasing the amount of banana skin powder is more effective. Alrshoudi *et al.* [31]) have developed pre-packed aggregate fibre-reinforced concrete reinforced with polypropylene waste carpet fibres. Their findings indicated that adding waste, PP fibre will decrease the compressive strength but will enhance the concrete's impact strength energy absorption and ductility. Gopalartnam and Shah [32] experimented with evaluating the performance of various types of natural fibre materials to measure their impact resistance behaviour. Akin and Orhan [33]) concluded that the energy absorption of steel fibres when subjected to pressure loads is important to prevent abrupt and explosive structural collapses under dynamic loads and when subjected to static loads.

Afshari and Riahi [34] found that incorporating fibres in oil palm shell lightweight aggregate concrete improved its mechanical properties, including compressive strength, tensile strength, and flexural strength. Riahi and Razaqpur [35] studied the performance of oil palm shell lightweight aggregate concrete reinforced with steel and synthetic fibres. They discovered that adding fibres enhanced the concrete's crack resistance and post-cracking behaviour. Mo *et al.* (2014) [36] studied the compressive strength of

crushed oil palm shell concrete with 1.0% steel fibre, control, and 1% PP fibre is 46.6 MPa, 42.9 MPa, and 26.8 MPa, respectively. Steel fibre enhanced the compressive strength, while PP reduced it. All OPS concrete with fibres had higher first crack impact energy than the control OPSC without fibre. The specimens with hybrid fibres (0.9%steel+0.1%PP) produced the highest impact resistance. Other researchers' results also indicate that including oil palm shells improves the impact resistance of lightweight concrete [37, 38, 39].

Impact resistance is a critical property determining the concrete's ability to withstand repetitive impacts while absorbing energy without experiencing cracking or spalling. Impact events are categorized into either low-velocity or high-velocity impacts. In their study, Mahmoud and Afroughsabet [40] elucidate the simplicity of the drop weight impact test, recommended by the ACI Committee 544 [41] as the most straightforward option among the various testing methods available. However, it is not a suitable test for a non-homogenous concrete composite with a non-uniform fibre distribution, mesh reinforcement, or having different boundary conditions. Xu et al. [42] conducted experimental drop-weight tests on concrete specimens reinforced with seven distinct types of fibres. The objective was to evaluate the impact resistance properties of the most effective fibre types. The propagation of tensile waves reflected from the point of impact has the potential to induce cracking on the rear surface of concrete.

Additionally, internal spalling within the concrete can be manifested in certain cases. Punching shear failure can be manifested in heavily reinforced slabs, although they exhibit substantial energy resistance. The localized crushing damage primarily attributed to compression failure can also be observed at the point impact [43].

Other similar studies also investigate the impact resistance of lightweight concrete incorporating oil palm shells as coarse aggregates and using fibres as reinforcement. The findings reveal that the addition of fibres enhances the impact resistance of the lightweight oil palm shell concrete (Md Akhir et al., 2020; Tahir et al., 2019; Liew et al., 2021; Yew et al., 2018) [44,45,46,47].

However, no research investigates the impact resistance performance of lightweight OPS concrete reinforced with hybrid polypropylene fibres and extruded polypropylene mesh with different fibre distributions.

There is a research gap in studying the effect of fibre distribution with mesh reinforcement on the impact resistance of lightweight concrete. The objective of this paper is to study the relationship of impact resistance of lightweight OPS-reinforced concrete slab reinforced with the hybrid Polypropylene (PP) fibres - PP mesh reinforcement with top and bottom fibre distribution against the different percentages of fibre volume fraction (VF) and its failure modes.

2 Materials

Oil palm shells, as illustrated in Figure 1, possess distinctive physical characteristics with a lightness in mass making them a viable alternative in producing lightweight concrete. The OPS aggregates of size range between 8mm and 10mm are sieved in this research.



Fig. 1: ops Lightweight Aggregates (8 – 10 mm Size)

Ordinary Portland cement of ASTM Type I and a 0.45 water-cement ratio is employed in a mixed design. The silica fume provided by EIKEM has a specific gravity of 2.2 and a particle size measuring 0.15 μm . Sika Viscocrete-15RM superplasticizer was with a dosage of 2% by weight of cement. The specific gravity of the superplasticizer used in this experiment is 1.12. The slump for the control is 130mm for medium workability fresh concrete with an oven density of 1905 kg/m^3 . The slump and oven dry density for PP3, PP2, and PP1 ranges from 10mm - 50 mm and 1580 – 1825 kg/m^3 , respectively.

In the mix design of OPS-LWC for the control and PP fibre volume fraction (VF), percentages of 1%, 2%, and 3% were used with its compressive strength as given in Table 1.

Table 1: Mixed Design and Compressive Strength

Mix Code (Fibre)	Binder		Aggregate		PP		Water		SP		Slump Mm	Oven Dry Density kg/m^3	Compressive Strength MPa
	Cement (kg)	SilicaFume (kg)	OPS (kg)	Sand (kg)	PP Fibre (VF%)	PP Fibre (kg)	Wt (kg)	w/c	Wt (gm)%	%			
Control	530	26.5	200	795	0	-	212	0.4	9.2	2	130	1905	30.3
PP1	530	26.5	200	795	1	0.612	212	0.4	9.2	2	75	1825	26.6
PP2	530	26.5	200	795	2	1.224	212	0.4	9.2	2	45	1700	23.5
PP3	530	26.5	200	795	3	1.836	212	0.4	9.2	2	20	1580	22.4

Extruded polypropylene mesh with 35 mm x 35 mm openings with a diameter of 2 mm is shown in Figure 2a. The mesh was cut to a square of 300 mm x 300 mm and placed at the mid-depth of the slab. Mega Mesh 1 fibrillated PP fibres of 19 mm length with an aspect ratio of 1188 and a tensile strength of 400MPa, as shown in Figure 2b.

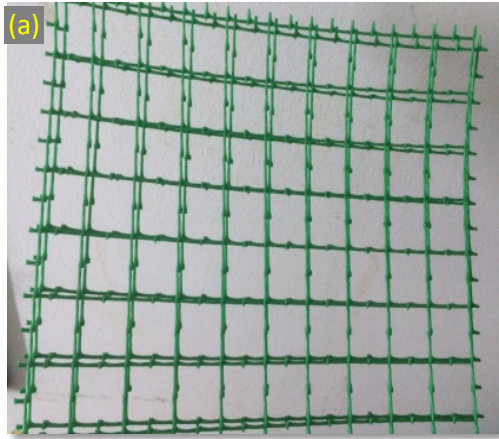
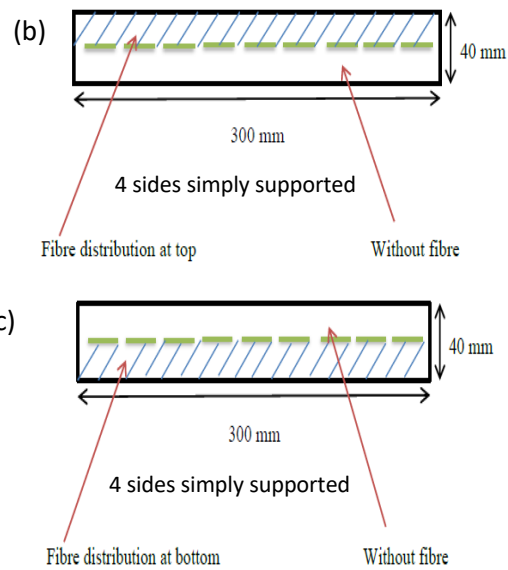
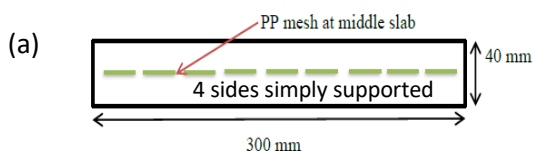


Fig. 2: Type of PP Reinforcement (a) PP Mesh Netting (35mm x 35mm x 2 mm diameter) and (b) Fibrillated PP fiber (19 mm length)

3 Methodology

3.1 Preparation of specimens

The configurations of the bottom and top PP fibre distribution with a PP mesh are shown in Figure 3. The sample has a control without fibre (Figure 3a). PP fibre distribution is randomly distributed at the top half of the slab (Figure 3b) and the bottom mid-half of the slab section (Figure 3c). All the slabs are reinforced with extruded PP mesh at the middle section.



(a) Control (without PP Fibre), (b) Top Fibre Distribution, and (c) Bottom Fibre Distribution

Fig. 3: Configuration of the Bottom and Top Fibre Distribution

Before mixing, the OPS lightweight aggregates were pre-soaked for 24 hours in water and surface dry from any excess water to achieve a state of saturated surface dryness. Then, the cement is put into the mixer with the OPS aggregates and uniformly mixed for 3 minutes. The remaining mixing amount of water containing SP was put into the mixer and mixed for an additional 5 minutes. The precisely measured weight of PP fibres is then manually dispersed into the mixture and mixed for another 4 minutes to obtain a uniform distribution. The finished mix is then cast into the formwork and compacted, as indicated in Figure 4a. After 24 hours, the slabs are removed from the formwork and cured in the water for 28 days. A whitewash paint is applied to the surface before the impact testing, as shown in Figure 4b.



(a) Casting of slabs



(b) Surface white wash with paint.

Fig. 4: Preparation of the Slab Specimens

3.2 Test setup and testing of specimens

In the research, a low-velocity drop-weight impact was carried out using a steel ball of 1.05 kg weight. The ball was dropped at a height of 0.300 m onto a specimen measuring 300mm square and a thickness of 40 mm. This specimen was placed on a square steel rack frame supported on all four sides, as illustrated in Figure 5.



Fig. 5: Impact Test Rig

At the service (first) crack and ultimate (failure) crack, the total crack length, width, and depth were measured by filler gauge with the total number of blows recorded. Each data point is taken from the average of three (3) specimen readings.

Table 2: contains the specification of the test specimens and the number of samples required for the experimental works.

Mix Code	PP Fibre VF %	PP Mesh	Fibre Distribution	No Slab Specimen Tested
Control	0%	Yes	-	3
PP1-Top	1%	Yes	Top	3
PP1-Bottom	1%	Yes	Bottom	3
PP2-Top	2%	Yes	Top	3
PP2-Bottom	2%	Yes	Bottom	3
PP3-Top	3%	Yes	Top	3
PP3-Bottom	3%	Yes	Bottom	3

21 sample slabs were cast and tested for the control and PP fibre of 1%, 2%, and 3% VF for top and bottom fibre distributions.

3.3 Theoretical Analysis

The falling body's potential energy is converted into strain energy at impact, which generates stresses within the target element, causing the formation of cracks. These cracks' characteristics, width, depth, length, and mode of failure are directly linked to the energy's intensity, amount of energy absorbed, and concrete properties. In this regard, the calculated energy is assumed to be entirely absorbed by the specimens.

The relationship between the potential energy of a drop-weight projectile and the strain energy dissipated in crack development is expressed as the following formula.

$$e = m \times g \times h \tag{1}$$

$$Es = Ns \times e \tag{2}$$

$$Eu = Nu \times e \tag{3}$$

Where e = energy per blow (Joules), m = mass of steel ball (kg) g = 9.81 m/s², h = height of drop (m), Es = service impact energy (J), Eu = ultimate impact energy (J), Ns = No of blows at the first crack (service) and Nu = No of blows at failure (ultimate) crack.

Crack resistance was calculated using the following formulas, which were proposed by Kankam [48];

$$Rs = IEs / (lc \times dc \times wc) \tag{4}$$

$$Ru = IEu / (lc \times dc \times wc) \tag{5}$$

Where Rs = Service crack resistance (N/ mm²), Ru = ultimate crack resistance (N/ mm²), lc = total length of all cracks (mm), dc = maximum crack depth (mm) and wc = maximum crack width (mm).

Another dimensionless factor is to measure the ultimate crack resistance against the compressive strength of the concrete given as a ratio. It measures the effectiveness of the crack resistance performance against its compressive strength.

Service and Ultimate impact crack resistance ratio were also defined by Equation 6 and Equation 7, respectively;

$$Cr = R_s / f_{cu} \tag{6}$$

$$Cr = R_u / f_{cu} \tag{7}$$

C_r = Impact crack resistance ratio, R_s = Service crack resistance (N/mm²), R_u = ultimate crack resistance (N/mm²), and f_{cu} = cube compressive strength of the concrete slab.

To easily evaluate quantitatively the improvement in the impact resistance characteristics, the impact residual strength ratio (I_{RS}) was formulated as the ratio of ultimate impact energy over service impact energy as given in Equation 8 (Ramakrishna and Sundararajan, 2005);

$$I_{RS} = E_u / E_s \tag{8}$$

I_{RS} = Impact strength ratio, E_s = service impact energy (J), E_u = ultimate impact energy (J).

The impact residual strength ratio helped to evaluate the post-crack behaviour of the composites easily and could also be taken as a measure of the ductility of the composite imparted by the fibre incorporated into the matrix.

4 Results and discussion

The details of the experimental impact test results and analysis for the impact energy, crack resistance, crack resistance ratio, and impact residual strength are given in Appendix 1. These data are used to tabulate the impact behaviour against the fibre VF and its fibre distributions.

4.1 Compressive Strength Relationship with Fibre VF%

Figure 6 shows the relationship between compressive strength f_{cu} against the percentage of fibre volume fraction, VF%.

The control has the highest compressive strength of 30.3 MPa. When the PP fibre content varied from 0% to 3.0% VF, the 28-day compressive strength decreased from 30.3 MPa to 22.4 MPa. It is evident that adding the PP fibre at a high dosage has a negative effect on the compressive strength due to fibre-to-fibre interaction can hinder the flow of the cement paste and cause localized stress concentrations; the balling effect may create voids and weaken the interfacial bond between the fibres and the cement paste, low workability may cause compaction problem, and it becomes more challenging to ensure proper fibre orientation throughout the concrete at higher fibre dosages. All these factors can lead to reduced load transfer efficiency and decreased compressive strength. The rate of decrease in compressive strength is 3.03 MPa with an

increase of 1% VF.

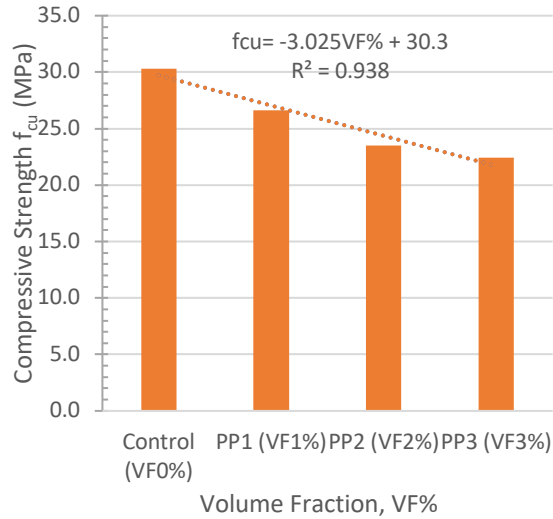


Fig. 6: Relationship between Compressive Strength, f_{cu} against Fibre VF%

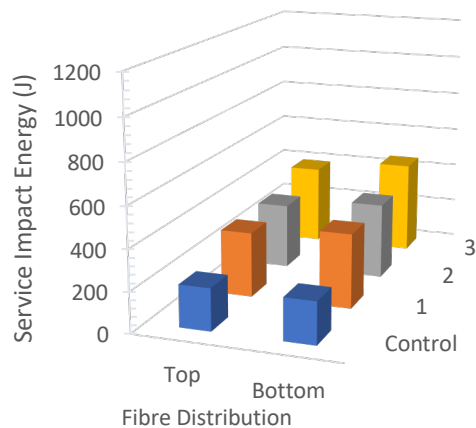
The incorporation of PP fibres in cement-based composites reduces their compressive strength. A similar trend has been confirmed by other researchers [49, 50, and 51]. It is a widely accepted understanding that the primary role of fibres is to control the crack propagation by bridging effect across cracks and enhanced post-cracking ductility rather than merely enhancing the compressive strength.

There is a good linear relation with an R^2 value of 0.938 between the compressive strength and the volume fraction of PP fibre as follows;

$$f_{cu} = -3.025VF\% + 30.3 \text{ with } R^2 = 0.938 \tag{9}$$

4.2 Impact Energy

Figure 7: shows the histogram plot between the service and ultimate impact energy against the percentage of fibre VF for top and bottom fibre distribution.



(a) Service Impact Energy

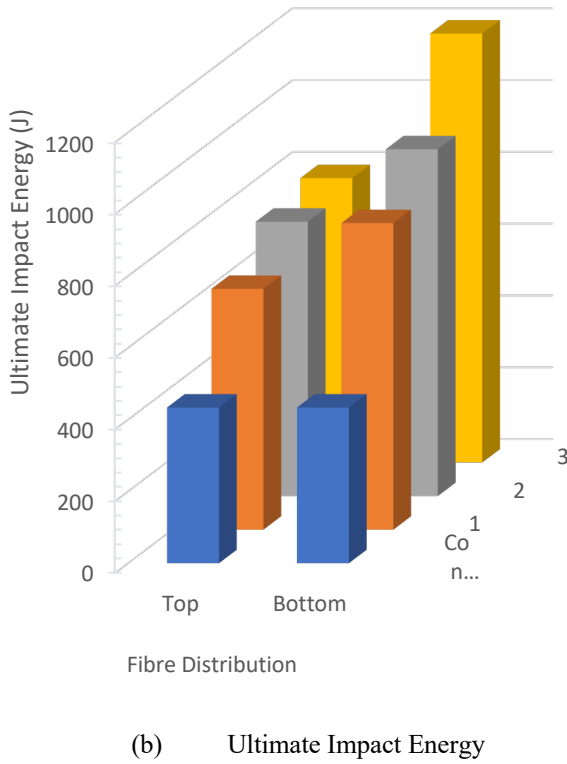


Fig. 7: Service and Ultimate Impact Energy against Fibre VF% for Top and Bottom Fibre Distribution

As the dosage of PP fibres increases, the capacity of slab specimens to absorb both service and ultimate impact energy increases. In simpler terms, augmenting the amount of PP fibres will enhance the load transfer mechanism from the matrix to the fibres. An increased bridging effect across cracks subsequently increases the energy absorption. The results indicate that slabs with PP fibre 3% VF dosage have the highest service impact energy value, 457.4 J, about 2.2 times higher than the control for bottom distribution, and 394.5 J, about 1.9 times higher than the control for top fibre distribution. The bottom fibre distribution with 1%, 2%, and 3% VF of PP fibre has a higher service impact energy of about 15% than the top fibre distribution. The maximum increase rate was in the slab when the PP fibre increased from 0% to 1% VF.

Slabs with PP fibre 3% VF dosage have the highest ultimate impact energy value, 1194.9 J, about 2.8 times higher than the control for bottom distribution, and 792.1 J, about 1.8 times higher than the control for top fibre distribution. The maximum increase rate was in the slab when the PP fibre increased from 0% to 1% VF. The bottom fibre distribution with 1%, 2%, and 3% VF of PP at ultimate impact energy fibre is higher by 27%, 26%, and 51%, respectively, than the top fibre distribution.

Figure 8 shows the relationship between service and ultimate impact energy against fibre volume fraction percentage.

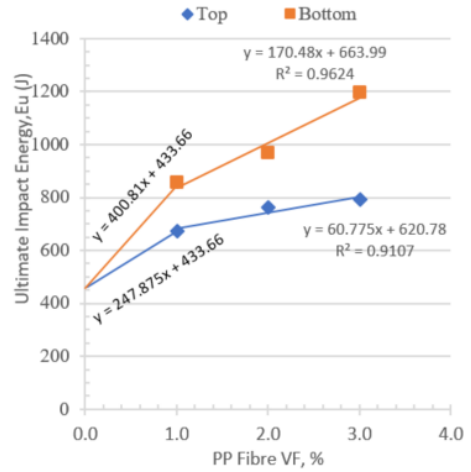
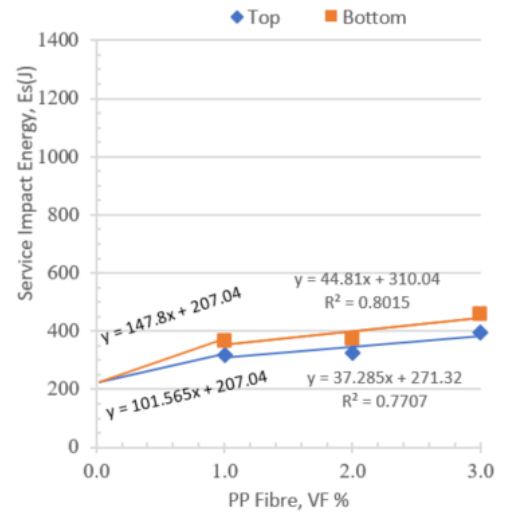


Fig. 8: Relationship between (a) Service and (b) Ultimate Impact Energy against Fibre VF%

The bi-linear correlation for service impact energy (E_s) against the volume fraction of PP fibre are as follows;

i) Top Fibre Distribution

$$\begin{aligned}
 &VF\% < 1.0: \\
 &E_{S(TOP)} = 01.565VF + 207.04 \quad \text{with } R^2 = 0.7707 \\
 &VF\% \geq 1.0: \\
 &E_{S(TOP)} = 37.285VF + 271.32 \quad \text{with } R^2 = 0.7707 \quad (10)
 \end{aligned}$$

ii) Bottom Fibre Distribution

$$\begin{aligned}
 &VF\% < 1.0: \\
 &E_{S(BOTTOM)} = 147.8VF + 207.04 \quad \text{with } R^2 = 0.8015 \\
 &VF\% \geq 1.0: \\
 &E_{S(BOTTOM)} = 44.81VF + 310.04 \quad \text{with } R^2 = 0.8015 \quad (11)
 \end{aligned}$$

The bi-linear correlation for ultimate impact energy (E_u)

against the volume fraction of PP fibre is as follows;

i) Top Fibre Distribution

VF% < 1.0:

$$Eu_{(TOP)} = 47.875VF + 433.66$$

VF% ≥ 1.0:

$$Eu_{(TOP)} = 60.775VF + 620.78 \text{ with } R^2 = 0.9107 \quad (12)$$

ii) Bottom Fibre Distribution

VF% < 1.0:

$$Eu_{(BOTTOM)} = 400.81VF + 433.66$$

VF% ≥ 1.0:

$$Eu_{(BOTTOM)} = 170.48VF + 663.99 \text{ with } R^2 = 0.9624 \quad (13)$$

The service increase rate and ultimate impact energy is higher when the fibre volume fraction is less than 1%. The bottom fibre distribution performs better than the top fibre distribution for the service and ultimate impact energy.

4.2. Crack Resistance

Figure 9 shows the 3-D histogram plot between the service and ultimate crack resistance against the percentage of fibre VF for top and bottom fibre distribution.

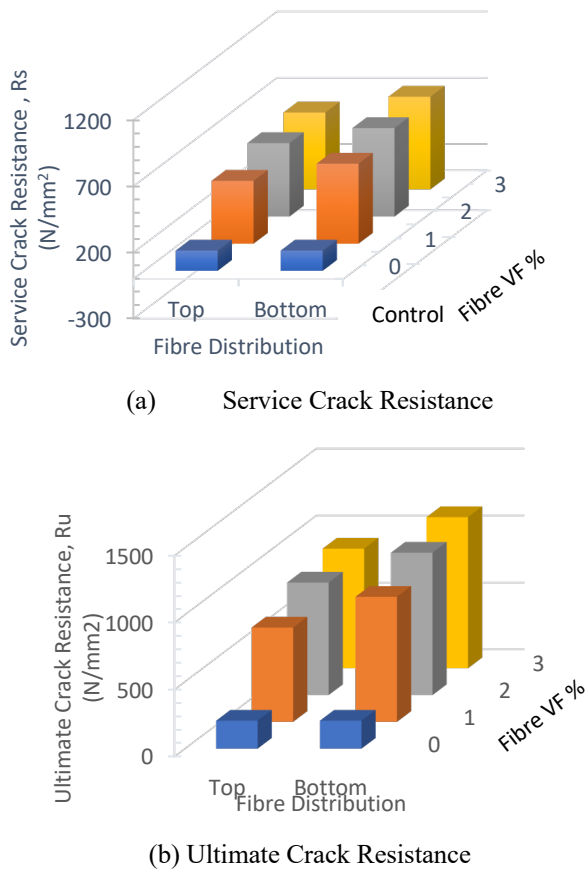


Fig. 9: Service and Ultimate Crack Resistance against Fibre VF% -Top and Bottom Fibre Distribution

The service and ultimate crack resistance of slab specimens increased with increased volume fraction of PP fibre. The results indicate that slabs with PP fibre 3% VF dosage have the highest service crack resistance value, 699.7 N/mm², about 4.6 times higher than the control for bottom distribution and 580.5 N/mm², about 3.8 times higher than the control for top fibre distribution as shown Figure 5(a). The bottom fibre distribution for 1%, 2%, and 3% VF of PP fibre have higher service crack resistance of 27%, 20%, and 21%, respectively, than the top fibre distribution.

Slabs with PP fibre 3% VF dosage have the highest ultimate crack resistance value, 1128 N/mm², about 5.4 times higher than the control for bottom distribution and 892.8 N/mm², about 4.3 times higher than the control for top fibre distribution as shown Figure 5(b). The bottom fibre distribution with 1%, 2%, and 3% VF of PP at ultimate crack resistance is higher by 33%, 27%, and 26%, respectively, than the top fibre distribution.

Figure 10 shows an excellent bi-linear correlation between service crack resistance (Rs) and ultimate crack resistance (Ru) for different volume fractions of PP fibre for both top and bottom fibre distribution with a minimum R² value of 0.9209.

The bi-linear correlation for service crack resistance (Rs) against the volume fraction of PP fibre are as follows;

i) Top Fibre Distribution

VF% < 1.0:

$$R_{s(TOP)} = 331.3VF + 152.6$$

VF% ≥ 1.0:

$$R_{s(TOP)} = 52.8VF + 431.03 \text{ with } R^2 = 0.9209 \quad (14)$$

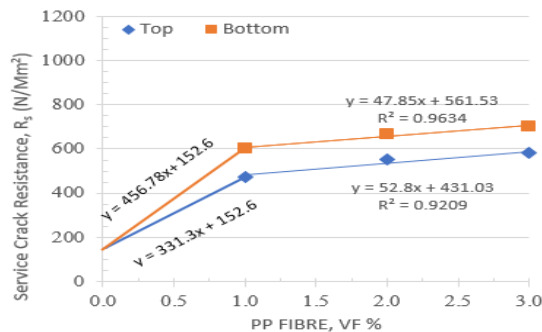
ii) Bottom Fibre Distribution:

VF% < 1.0:

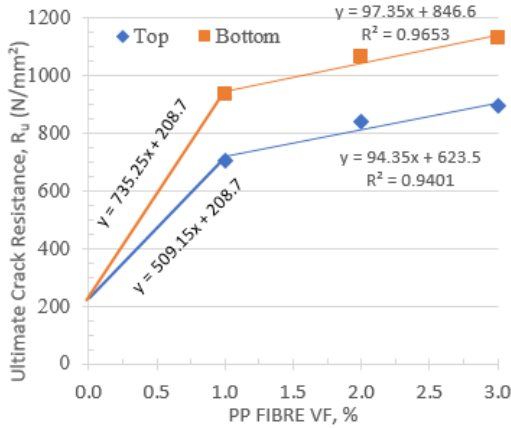
$$R_{s(BOTTOM)} = 456.78VF + 152.6$$

VF% ≥ 1.0:

$$R_{s(BOTTOM)} = 47.85VF + 561.53 \text{ with } R^2 = 0.9634 \quad (15)$$



(a) Service Crack Resistance



(b) Ultimate Crack Resistance

Fig. 10: Relationship between (a) Service and (b) Ultimate Crack Resistance against Fibre VF%

The bi-linear correlation for ultimate crack resistance (R_u) against the volume fraction of PP fibre is as follows;

i) Top Fibre Distribution

$VF\% < 1.0$:

$$R_{s(TOP)} = 509.15VF + 208.7$$

$VF\% \geq 1.0$:

$$R_{u(TOP)} = 94.35VF + 623.5 \text{ with } R^2 = 0.9401 \quad (16)$$

ii) Bottom Fibre Distribution:

$VF\% < 1.0$:

$$R_{s(BOTTOM)} = 735.25VF + 208.7$$

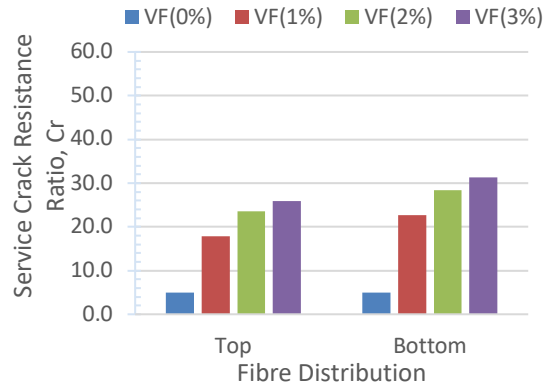
$VF\% \geq 1.0$:

$$R_{u(BOTTOM)} = 97.35VF + 846.6 \text{ with } R^2 = 0.9653 \quad (17)$$

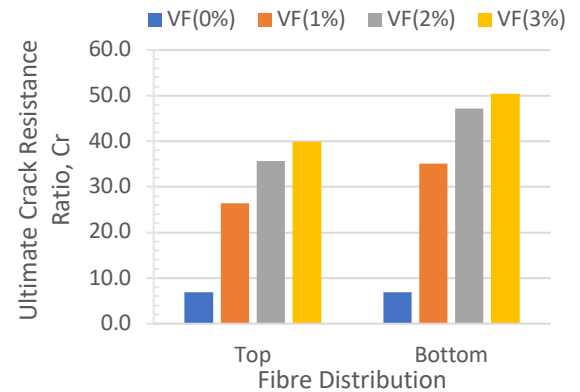
The rate of increase of the service and ultimate crack resistance is higher when the fibre volume fraction is less than 1%. The bottom fibre distribution performs better in the crack resistance than the top fibre distribution under the service and ultimate crack resistance condition.

4.3. Crack Resistance Ratio

Figure 11 shows the service and ultimate crack resistance ratio (C_r) against fibre VF% for bottom and top fibre distribution. The service C_r for bottom fibre distribution with 1%, 2%, and 3% VF of PP fibre is 27%, 20%, and 20%, respectively, higher than top fibre distribution. The bottom fibre distribution with 1%, 2%, and 3% VF of PP at the ultimate C_r is 32%, 32%, and 26%, respectively, higher than the top fibre distribution. The bottom fibre distribution has a higher C_r value than the top distribution; as such bottom fibre is more effective than the top fibre in increasing the C_r of the slab under service and ultimate crack conditions.



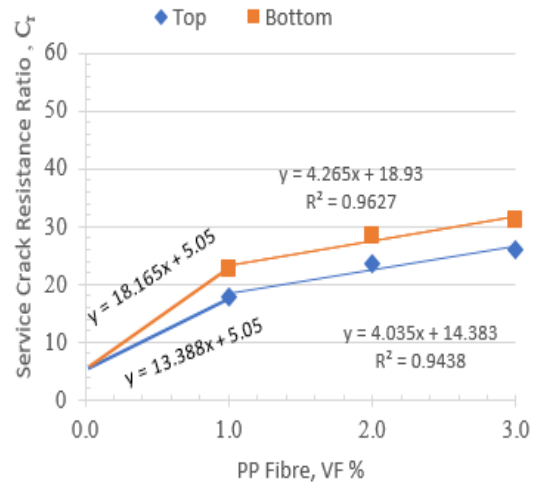
(a) Service Crack Resistance Ratio



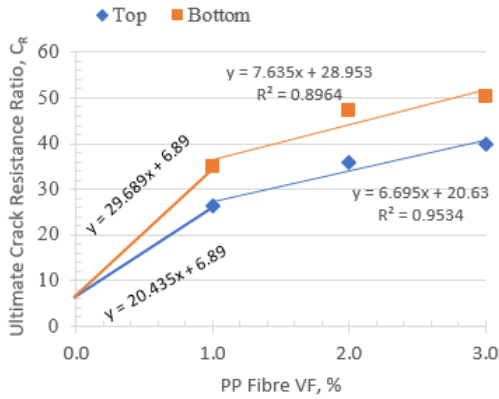
(b) Ultimate Crack Resistance Ratio

Fig. 11: Service and Ultimate Crack Resistance Ratio, C_r against fibre VF%

Figure 12 shows an excellent bi-linear correlation between the service C_r and ultimate C_r for different volume fractions of PP fibre for both top and bottom fibre distribution with a minimum R^2 value of 0.8964.



(a) Service Crack Resistance Ratio



(b) Ultimate Crack Resistance Ratio

Fig. 12: Relationship between (a) Service and (b) Ultimate Crack Resistance Ratio against Fibre VF%

The bi-linear relationship of service crack resistance ratio (Cr_s) against the volume fraction of PP fibre is as follows;

i) Top Fibre Distribution

$VF\% < 1.0$:

$$Cr_{s(TOP)} = 13.388VF + 5.05$$

$VF\% \geq 1.0$:

$$Cr_{s(TOP)} = 13.388VF + 5.05 \quad \text{with } R^2 = 0.9438 \quad (18)$$

ii) Bottom Fibre Distribution:

$$Cr_{s(BOTTOM)} = 18.165VF + 5.05$$

$VF\% \geq 1.0$:

$$Cr_{s(BOTTOM)} = 4.265VF + 18.93 \quad \text{with } R^2 = 0.9627 \quad (19)$$

The bi-linear relationship of the ultimate crack resistance ratio (Cr_u) against the volume fraction of PP fibre is as follows;

i) Top Fibre Distribution

$VF\% < 1.0$:

$$Cr_{u(TOP)} = 20.435VF + 6.89$$

$VF\% \geq 1.0$:

$$Cr_{u(TOP)} = 6.695VF + 20.63 \quad \text{with } R^2 = 0.9534 \quad (20)$$

ii) Bottom Fibre Distribution:

$VF\% < 1.0$:

$$Cr_{u(BOTTOM)} = 29.689VF + 6.89$$

$VF\% \geq 1.0$:

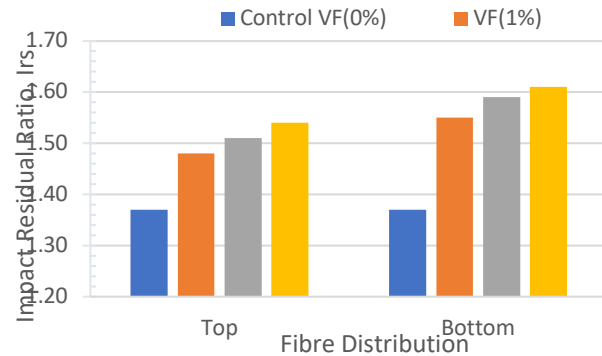
$$Cr_{u(BOTTOM)} = 7.635VF + 28.953 \quad \text{with } R^2 = 0.8964 \quad (21)$$

The rate of increase of the service and ultimate crack resistance ratio is higher when the fibre volume fraction is less than 1%. The bottom fibre distribution performs

better than the top fibre distribution for the service and ultimate crack resistance ratio.

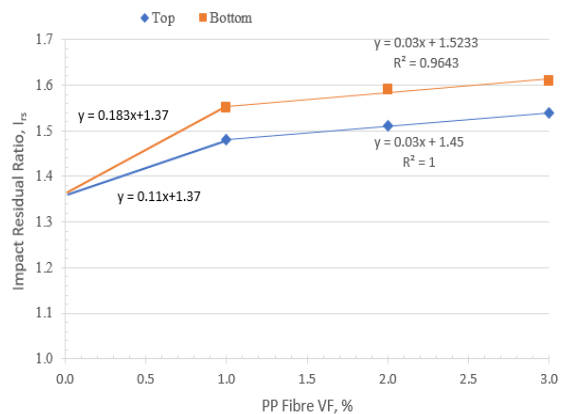
4.4. Impact Residual Strength Ratio

Figure 13 shows the impact residual strength ratio and fibre VF% for top and bottom distribution.

**Fig. 13:** Impact Residual Ratio, I_{RS} , and Fibre VF% for Top and Bottom Distribution

The residual impact strength ratio (I_{RS}) was found to vary from 1.37 to 1.54 for top fibre distribution and 1.37 to 1.61 for bottom fibre distribution with different VF% of PP fibre. It was obvious that the more PP fibre content, the higher the impact residual strength ratio, which showed that the ductility of the slab was increased. The bottom fibre distribution has higher I_{RS} values than the top distribution; as such bottom fibre is more effective than the top fibre in increasing the ductility of the slab. The slab offered the maximum I_{RS} of 1.61 with 0.3% VF of PP fibre for the bottom distribution. The bottom fibre is more effective in increasing the ductility than the top fibre distribution by about 5% for each fibre VF%.

Figure 14 shows an excellent bi-linear correlation between impact residual ratio (I_{RS}) for different volume fractions of PP fibre for both top and bottom fibre distribution with a minimum R^2 value of 0.8964.

**Fig. 14:** Relationship between Impact Residual Ratio, I_{RS} against Fibre VF%

The bi-linear relationship of impact residual ratio (I_{RS}) against the volume fraction of PP fibre is as follows;

i) Top Fibre Distribution

$VF\% < 1.0$:

$$I_{RS(TOP)} = 0.11VF + 1.37$$

$VF\% \geq 1.0$:

$$I_{RS(TOP)} = 0.003VF + 1.45 \quad \text{with } R^2 = 1 \tag{22}$$

ii) Bottom Fibre Distribution:

$VF\% < 1.0$:

$$I_{RS(BOTTOM)} = 0.183VF + 1.37$$

$VF\% \geq 1.0$:

$$I_{RS(BOTTOM)} = 0.03VF + 1.5233 \quad \text{with } R^2 = 0.9643 \tag{23}$$

The rate of increase of the impact residual ratio is higher when the fibre volume fraction is less than 1%. The bottom fibre distribution has better post-cracking ductility than the top fibre distribution with a higher impact residual ratio.



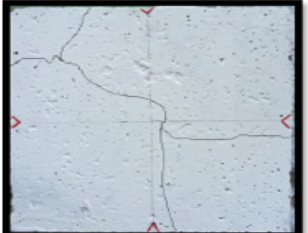


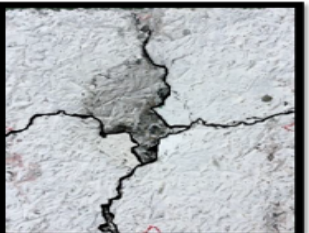
4.4 Failure Modes

Impact load at the frontal face results in the concrete's tensile cracking and spalling on the distal face.

This happens due to reflected tensile waves propagating from the point of impact. Upon impact, localized damage is also noticed at the point of contact at the frontal face. This damage may be due to compression failure near the point of contact causing the crushing of the concrete. Overly reinforced concrete slabs may fail due to punching shear without segmented failure zones. Generally, cracks will propagate from the centre to the edge of the distal face under tensile stress. A crack propagates and approaches a fibre, triggering de-bonding at the fibre-matrix interface due to the tensile stresses along the crack's path. Once the crack reaches this interface, there is a reduction in the stress at its tip. This circumstance acts to impede further the propagation of the crack. This phenomenon characterizes concrete's bridging effect or crack-curtailling capability when reinforced with fibres, as highlighted in references [53, 54, 55]. The process by which fibres deter crack proliferation is accomplished by connecting the crack faces by the bridging effect. After that, as the load increases, the PP fibres fail through complete pullout and fibres tensile failure. The PP mesh netting is still intact but fully elongated, preventing the sudden collapse at the ultimate impact load.

The segmental failure modes of the hybrid PP fibre – PP mesh netting for the service and ultimate crack resistance are shown in Table 3.

Table 3: Failure modes of the hybrid PP Fibre – PP Mesh at service and ultimate impact loads

No	Samples	Service Crack	Ultimate Crack	Remark
1	Control Without fibre Slab thickness = 40mm 4 Support PP mesh in the middle			-Crack starts at distal face N(s) = 69 blows N(u) = 143 blows -In the failure stage 4 segmental zones were generated -
2	Volume fraction = 3% Slab thickness = 40mm PP mesh in the middle 4 -way support condition Fibre distribution at top			-Crack starts at distal face N(s) = 129 blows N(u) = 257 blows -In the failure stage 5 segmental zones were generated
3	Volume fraction = 3% Slab thickness = 40mm PP mesh in the middle 4 -way support condition Fibre distribution at bottom			-Crack starts at distal face N(s) = 147 blows N(u) = 386 blows -In the failure stage 4 segmental zones were generated

Top fibre distribution for 3% VF increases the mode of segmental failures to 4 and 5 numbers compared to the bottom fibre distribution of only 3 and 4 numbers under service and ultimate cracks. Similar patterns have been observed with 1%VF and 2%VF; however, the number of segmental failures for 1%VF is less than 2%VF, and 2%VF is similar to 3%VF. Top fibres have better crack dispersion control than the bottom fibres, although their crack resistance is lower. Bottom fibres have better resistance against tensile failures, resulting in higher crack resistance than the top fibre distribution. The control's segmental failure zones are generally less than the slab with fibres under service and ultimate crack conditions. It is observed that the random fibre distribution with a greater fraction volume at the top and bottom region of the slab exhibited a higher number of segmental failures along the fracture zone, accompanied by an increase in micro-cracking at the other regions of the slab in contrasted with areas possessing a lower fraction volume.

Figure 15 shows the action of the PP fibre and PP mesh reinforcement at the service (initial) phase and ultimate (failure) phase under impact load.

The fibres serve the vital function of bridging micro cracks, thereby exerting controls over their coalescence, while the mesh reinforcement fulfils the role of bridging the macro-cracks, thus inhibiting the propagation of micro cracks.

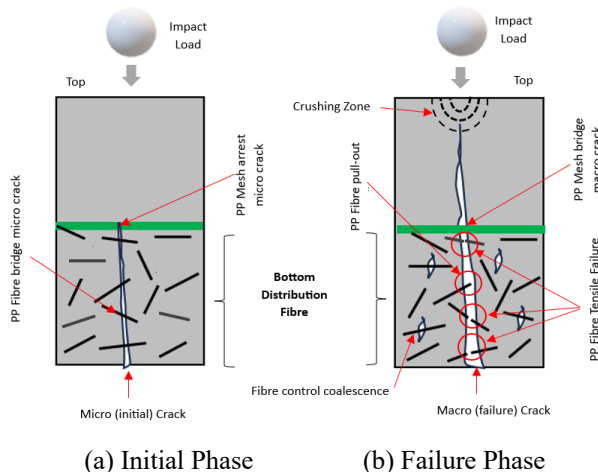


Fig. 15: Action of the PP fibre and PP mesh reinforcement (a) Initial Phase and (b) Failure Phase

Crushing zones at the point of contact in the centre of the slab area due to compression failure are observed for all the specimens under the condition of the ultimate cracks. It is observed that the PP fibre controls the micro-cracks while the PP mesh arrests the minor crack at the initial phase. The PP fiber's pullout and tensile failure occur at the failure phase, and the PP mesh bridges the macro crack.

They control the micro-crack, and macro-crack results in higher strength and substantially improved impact crack resistance. As a result of this synergetic mechanism, ductility enhancement of the slab under impact load will be

increased.

5 Conclusions

This study evaluates the effect of fibre distribution on the impact behaviour of lightweight OPS concrete. The relationship of impact resistance of lightweight OPS-reinforced concrete slab reinforced with the hybrid PP fibres - PP mesh reinforcement with top and bottom fibre distribution against the different percentages of VF and its failure modes have been established. The results with the proposed equations indicate that an increase in PP fibre dosage significantly increases all the impact factors and its post-cracking ductility behaviour. The bottom fibre distribution performs better than the top fibre distribution in all the above impact factors. The breakdown of the conclusion according to the objective is as given below;

1. The bottom fibre distribution with 1%, 2%, and 3% VF of PP fibre has a higher service impact energy of about 15% than the top fibre distribution. The bottom fibre distribution with 1%, 2%, and 3% VF of PP at ultimate impact energy fibre is higher by 27%, 26%, and 51%, respectively, than the top fibre distribution.
2. The bottom fibre distribution for 1%, 2%, and 3% VF of PP fibre has higher service crack resistance of 27%, 20%, and 21%, respectively, than the top fibre distribution. The bottom fibre distribution with 1%, 2%, and 3% VF of PP at ultimate crack resistance is higher by 33%, 27%, and 26%, respectively, than the top fibre distribution.
3. The service crack resistance ratio for bottom fibre distribution with 1%, 2%, and 3% VF of PP fibre is 27%, 20%, and 20%, respectively, higher than top fibre distribution. The bottom fibre distribution with 1%, 2%, and 3% VF of PP at the ultimate crack resistance ratio is 32%, 32%, and 26%, respectively, higher than the top fibre distribution.
4. The impact residual strength ratio of the slabs with 1%, 2%, and 3% VF of PP fibre for the bottom distribution is higher by 5%, 3%, and 5%, respectively than the top distribution fibre.
5. There were excellent bi-linear equations between the impact behaviour against the PP fibre volume fraction with a minimum R^2 value of 0.8964. Bottom fibre distribution is more efficient in impact resistance than the slab with top fibre distribution and without fibre (control). Increasing the dosage of PP fibre increases its impact resistance.
6. The top fibre distribution has more segmental failure zones than the bottom fibre distribution, although the bottom fibre distribution has better impact performance and post-cracking ductility behaviour. PP fibres control the micro-cracks at the initial phase, while the PP mesh bridges the minor cracks at the failure phase.

Acknowledgments

The authors would like to thank the INTI International University, Malaysia for the financial support of the publication of this article.

References

- [1] Thomas, H. R., & Fernando, S. C. (2019). Sustainable Construction Materials: Present Challenges and Future Opportunities. *Construction and Building Materials*, 213, 787-801.
- [2] Madurwara, M. V., Ralegaonkar, R. V., Mandavgane, S. A. (2013) Application of agro-waste for sustainable construction materials: A review, *Construction and Building Materials*, 38(2013)872–878.
- [3] Arunachalam, S., & Umarani, C. (2017). Use of palm kernel shell as lightweight aggregate in concrete: A review. *Construction and Building Materials*, 137, 271-280.
- [4] Hasan, A. R., Hussain, M. S., Faisal, A., Faruq, M. O., & Zilfiqar, A. (2020). Structural concrete using coconut shell waste as aggregate: A review. *Journal of Building Engineering*, 31, 101333.
- [5] Moa, K. H, Thomas, B .S., Yap, S. P., Abutaha, F., Tana, C. G. (2020). Viability of agricultural wastes as substitute of natural aggregate in concrete: A review on the durability-related properties, *Journal of Cleaner Production*, 275 (2020) 123062
- [6] Farahani, J. N., Shafiqh, P., Alsubari, B., Shahnazar, S., & Mahmud, H. B. (2017). Engineering properties of lightweight aggregate concrete containing binary and ternary blended cement. *Journal of Cleaner Production*, 156, 765-774.
- [7] Mahmud, H., Shafiqh, P., & Jumaat, M. Z. (2013). Structural lightweight aggregate concrete containing high volume waste materials. *Key Engineering Materials*, 594-595, 454-458.
- [8] Kareem, M. A., Raheem, A.A., Oriola, K. O., Abdulwahab,R. (2022), A review on application of oil palm shell as aggregate in concrete -Towards realising a pollution-free environment and sustainable concrete. *Environmental Challenges*, 8 (2022) 100531.
- [9] Aslam, M., Shafiqh, P., & Jumaat, M. Z. (2015). Structural lightweight aggregate concrete by incorporating solid wastes as coarse lightweight aggregate. *Applied Mechanics and Materials*, 747, 419-423.
- [10] Abdul Rahman, N., Tan, A. S. H., Waqbitu, F. and Roslan, N. H. (2020), The effectiveness of oil palm shell (OPS) as major aggregate replacement in concrete, *IOP Conf. Ser.: Earth. 476 (2020) 012-019. DOI 10.1088/1755-1315/476/1/012019.*
- [11] Mannan, M.A., Alexandra, J., Ganapathy, C., Teo, D.C.L., 2006. Quality improvement of oil palm shell (OPS) as coarse aggregate in lightweight concrete. *Build. Environ.* 41, 1239–1242.
- [12] Mo, K.H., Yap, S. P., Alengaram, U. J., Jumaat, M. Z., Bu, C. H. (2014). Impact resistance of hybrid fibre-reinforced oil palm shell concrete. *Construction and Building Materials*, 50(2014)499–507.
- [13] Maghfouri, M., Shafiqh, P., Aslam, M., 2018. Optimum oil palm shell content as coarse aggregate in concrete based on mechanical and durability properties. *Adv. Mater. Sci. Eng.* 4271497, 1–14. doi: 10.1155/2018/4271497.
- [14] Aslam, M., Shafiqh, P., Jumaat, M. Z. (2017). High strength lightweight aggregate concrete using blended coarse lightweight aggregate origin from palm oil industry. *Sains Malaysia* 46, 667-675. doi:10.17576/jsm-2017-4604-20.
- [15] Yap, S. P., Bu,C., Alengaram, U. J., Mo, K. H., Jumaat, M. (2014). Flexural toughness characteristics of steel–polypropylene hybrid fibre-reinforced oil palm shell concrete. *Materials & Design*, 57 (2014) 652–659.
- [16] Nili, M., Ghorbankhani, A. H., Alavinia, A., & Zolfaghari, M. (2016). Assessing the impact strength of steel fibre-reinforced concrete under quasi-static and high velocity dynamic impacts. *Construction and Building Materials*, 107, 264-271.
- [17] Hwang, C. L., Tran, V. A., Hong, J. W., & Hsieh, Y. C. (2016). Effects of short coconut fibre on the mechanical properties, plastic cracking behavior, and impact resistance of cementitious composites. *Construction and Building Materials*, 127, 984-992.
- [18] Cifuentes, H., García, F., Maeso, O., & Medina, F. (2013). Influence of the properties of polypropylene fibres on the fracture behavior of low-, normal-, and high-strength FRC. *Construction and Building Materials*, 45, 130-137.
- [19] Aliabdo, A. A. E., Abd Elmoaty & A. E. M., Hamdy, M. (2013). Effect of internal short fibres, steel reinforcement, and surface layer on impact and penetration resistance of concrete. *Alexandria Engineering Journal*. 2013;52, 407-417.
- [20] Saidani, M., Saraireh, D., & Gerges, M. (2016). Behaviour of different types of fibre reinforced concrete without admixture. *Engineering Structures*, 113, 328-334.
- [21] Bagherzadeh, R., Pakravan, H. R., Sadeghi, A., Latifi, M., & Merati, A. A. (2012). An investigation on adding polypropylene fibres to reinforce lightweight cement composites (LWC). *Journal of Engineered Fibres and Fabrics*, 7(4), 13-21.
- [22] Islam, M. T., & Bindiganavile, V. (2011). The impact

- resistance of masonry units bound with fibre reinforced mortars. *Construction and Building Materials*, 25(6), 2851-2859.
- [23] Mastali, M., & Dalvand, A. (2016). The impact resistance and mechanical properties of self-compacting concrete reinforced with recycled CFRP pieces. *Composites Part B: Engineering*, 92, 360-376.
- [24] Li, Y.-F., Lee, K.-F., Ramanathan, G. K., Cheng, T.-W., Huang, C.-H., & Tsai, Y.-K. (2021). Static and dynamic performances of chopped carbon-fibre-reinforced mortar and concrete incorporated with disparate lengths. *Materials*, 14(7), 1832.
- [25] Nia, A. A., Hedayatian, M., Nili, M., Sabet, V. A. (2012) An experimental and numerical study on how steel and polypropylene fibres affect the impact resistance in fibre-reinforced concrete *International Journal of Impact Engineering* 46 (2012) 62-73.
- [26] Yew, M. K., Mahmud, H. B., Ang, B. C., & Yew, M. C. (2015). Influence of different types of polypropylene fibre on the mechanical properties of high-strength oil palm shell lightweight concrete. *Construction and Building Materials*, 80, 277-284.
- [27] Kim, H. M., Yap, S. P., Alengaram, U. J., Jumaat, M. Z., & Bu, C. H. (2014). Impact resistance of hybrid fibre-reinforced oil palm shell concrete. *Construction and Building Materials*, 64, 156-163.
- [28] Islam, A., Alengaram, U. J., Jumaat, M. Z., Ghazali, N. B., Yusoff, S., & Bashar, I. I. (2017). Influence of steel fibres on the mechanical properties and impact resistance of lightweight geopolymer concrete. *Construction and Building Materials*, 134, 366-376S.
- [29] Zamzani, N. M., Mydin, A. O., & Ghani, A. N. A. (2018). Experimental investigation on engineering properties of lightweight foamed concrete (LFC) with coconut fibre addition. *MATEC Web of Conferences* 250, 05005 (2018).
- [30] Mohamad, N., Iman, M. A., Samad, A. A. A., Mydin, A. O., Jusoh, S., Sofia, A., ... & Lee, B. (2019). Flexure behaviour of foamed concrete incorporating banana skin powder and palm oil fuel ash strengthened with carbon fibre reinforced plate. *IOP Conference Series: Materials Science and Engineering*, 469(1), 012078.
- [31] Alrshoudi, F., Mohammadhosseini, H., Alyousef, R., Tahir, M. M., Alabduljabbar, H., & Mohamed, A. M. (2020). The impact resistance and deformation performance of novel pre-packed aggregate concrete reinforced with waste polypropylene fibres. *Crystals* 2020,10,788
- [32] Gopalartnam, V.S. and Shah, S. P. (1986) Properties of fibre reinforced concrete subjected to impact loading. *ACI Journal*, 1986;83(1):117-26.
- [33] Akin, S. K., & Orhan, M. (2023). The Effect of Steel Fibres on the Interlocking Length between Reinforcement and Concrete and on Compressive Strength of Concrete. *Advances in Civil Engineering*, vol. 2023, Article ID 5535526, 11 pages, 2023. <https://doi.org/10.1155/2023/5535526>
- [34] Afshari, M., & Riahi, S. (2018). Experimental investigation on the mechanical properties of fibre-reinforced concrete containing oil palm shell as lightweight aggregate. *Construction and Building Materials*, 178, 413-424.
- [35] Riahi, S., & Razaqpur, A. G. (2018). Performance of oil palm shell lightweight aggregate concrete reinforced with steel and synthetic fibres. *Construction and Building Materials*, 164, 424-436.
- [36] Mo, K.H., Yap, S. P., Alengaram, U. J., Jumaat, M. Z., Bu, C. H. (2014). Impact resistance of hybrid fibre-reinforced oil palm shell concrete. *Construction and Building Materials*, 50(2014)499-507.
- [37] Md Din, M. F., Megat Johari, M. A., Shahidan, S., Mohd Nawi, M. N., & Ali, A. A. A. (2017). Impact Resistance of Lightweight Concrete with Oil Palm Shell Aggregate. *Key Engineering Materials*, 742, 30-35.
- [38] Mohd Nawi, M. N., Abdullah, N., Othman, N., & Shahidan, S. (2019). Impact Strength of Lightweight Concrete Reinforced with Oil Palm Shell. *Journal of Engineering Science and Technology*, 14(3), 1494-1506.
- [39] Nuruddin, M. F., Arshad, M. F., & Hassan, M. K. (2011). Mechanical Properties and Impact Resistance of Lightweight Concrete Containing Oil Palm Shell (OPS) Aggregate. *Construction and Building Materials*, 25(3), 1228-1233.
- [40] Mahmoud, N. and Afrouhsabet, V. (2010) Combined effect of silica fume and steel fibres on the impact resistance and mechanical properties of concrete. *International Journal of Impact Engineering* 37(2010) 879 – 886.
- [41] ACI Committee 544 (1996). State-of-the-art report on fibre-reinforced concrete. ACI Committee 544 report 544.1R-96. Detroit: American Concrete Institute; 1996.
- [42] Xu, Z., Hao, H., Li, H. N. (2012) Experimental study of dynamic compressive properties of fibre reinforced concrete materials with different fibres. *Material Design*, 2012;33:42-55.
- [43] Yahaghi, J., Che Muda, Z. and Beddu, S. (2016), Impact resistance of oil palm shells concrete reinforced with polypropylene fibre, *Construction and Building Materials*, 123 (2016) 394-403.

- [44] Md Akhir, M. F., Mohamed Sunar, N. A., & Jaafar, M. S. (2020). Impact Strength and Flexural Performance of Lightweight Oil Palm Shell Concrete Reinforced with Different Fibres. *Journal of Advanced Research in Materials Science*, 66(1), 16-25.
- [45] Tahir, M. F. M., Saleh, M. A. M., Ibrahim, N. M., & Abd Rahman, N. A. (2019). Impact Resistance and Mechanical Properties of Lightweight Oil Palm Shell Concrete with Polypropylene Fibres. *Construction and Building Materials*, 224, 117-126.
- [46] Liew, Y. M., Mohd Nawi, M. N., Megat Johari, M. A., & Ramli, M. (2021). Impact Resistance and Flexural Properties of Lightweight Concrete Reinforced with Oil Palm Shell and Steel Fibres. *Materials Today: Proceedings*, 44, 4236-4242.
- [47] Yew, M. C., Gan, B. H., Lim, Y. M., & Lee, S. K. (2018). Flexural and Impact Performance of Reinforced Lightweight Oil Palm Shell Concrete. *Journal of Advanced Concrete Technology*, 16(7), 323-335.
- [48] Kankam, C.K.(1999) Impact Resistance of palm kernel fibre-reinforced concrete pavement slab. *Journal of Ferrocement* 1999;29(4):279-86.
- [49] Abdollahnejad, Z., & Dabir, B. (2016). Effect of polypropylene fibres on the compressive and flexural strength of lightweight concrete. *Construction and Building Materials*, 124, 95-103.
- [50] Ganesan, N., & Rajagopal, K. (2017). Compressive and flexural behaviour of polypropylene fibre-reinforced lightweight aggregate concrete. *Construction and Building Materials*, 156, 871-877.
- [51] Khan, F. U., Su, S. K., & Aziz, F. N. (2018). Effect of polypropylene fibre volume on compressive strength of lightweight concrete. *IOP Conference Series: Materials Science and Engineering*, 344(1), 012059.
- [52] Rahmani, T., Kiani, B., Shekarchi, M., & Safari, A. (2012). Statistical and experimental analysis on the behavior of fibre reinforced concretes subjected to drop weight test. *Construction and Building Materials*, 37, 360-369. <http://dx.doi.org/10.1016/j.conbuildmat.2012.07.068>.
- [53] Song, P. S., Hwang, S., & Sheu, B. C. (2005). Strength properties of nylon- and polypropylene-fibre-reinforced concretes. *Cement and Concrete Research*, 35, 1546-1550.
- [54] Kakooei, S., Akil, H. M., Jamshidi, M., & Rouhi, J. (2012). The effects of polypropylene fibres on the properties of reinforced concrete structures. *Construction and Building Materials*, 27, 73-77. <http://dx.doi.org/10.1016/j.conbuildmat.2011.08.015>.
- [55] Han, C.-G., Hwang, Y.-S., Yang, S.-H., &

Gowripalan, N. (2005). Performance of spalling resistance of high-performance concrete with polypropylene fibre contents and lateral confinement. *Cement and Concrete Research*, 35, 1747-1753. <http://dx.doi.org/10.1016/j.cemconres.2004.11.013>.

Biography:



Zakaria Che Muda

earned his Ph. D. degree in Built Environment from University of Malaya. He is currently a Professor at the Department of Civil Engineering, INTI International University. He has published over 100 papers in international journals. His research interests are focused on fibre reinforced concrete,

lightweight concrete and impact resistance structures.



Agusril Syamsir

earned his Ph. D. degree in Structural Engineering from University Pertahanan Nasional Malaysia in 2013. He is currently a Senior Lecturer at the Department of Civil Engineering, University Tenaga Nasional. He has published about 150 papers in international conference

proceedings and journals. His research interests are focused on concrete composite, numerical analysis and impact resistance structures.



Md Ashrafal Alam

earned his Ph. D. in Structural Engineering from University of Malaya in 2010. He is currently a Professor at Department of Civil Engineering, University of Asia Pacific, Bangladesh. He has published about 71 papers in international conference

proceedings and journals. His research interests include retrofitting of structures and natural fibre laminates for structural strengthening.



As'ad Zakaria is currently a Ph. D student at the Institute of Energy Systems, School of Engineering, University of Edinburgh, Edinburgh, UK. He has published more than 10 papers in international journals. His research interest is in monte carlo simulation, electric vehicle, power system analysis and renewable

energy system.

Appendix 1: Experimental Results of Impact Test of Top and Bottom Fibre Distribution

Fibre VF%	Fibre Distribution	Sample No	Crack	N	wc (mm)	lc (mm)	dc (mm)	Impact Energy ¹ (Joule)	R ² (N/mm ²)	fcu (N/mm ²)	Cr ³	I _r ⁴
Control (0%)	-	1	Service	66	0.10	430	30	203.95	158.10	30.3	5.22	
			Ultimate	138	1.00	680	30	426.45	209.04	30.3	6.90	1.32
		2	Service	66	0.10	480	30	203.95	141.63	30.3	4.67	
			Ultimate	140	2.00	720	30	432.63	200.29	30.3	6.61	1.41
		3	Service	69	0.10	450	30	213.22	157.94	30.3	5.21	
			Ultimate	143	2.00	680	30	441.90	216.62	30.3	7.15	1.37
Average	Service	67.00	0.10	453.33	30	207.04	152.56	30.3	5.03			
Ultimate	140.33	1.67	693.33	30	433.66	208.65	30.3	6.89	1.37			
PP1-Top (VF1%)	Top	1	Service	102	0.15	430	30	315.20	488.68	26.6	18.37	
			Ultimate	219	1.00	630	30	676.75	716.14	26.6	26.92	1.47
		2	Service	52	0.15	460	30	324.47	470.25	26.6	17.68	
			Ultimate	216	2.00	600	30	667.48	741.65	26.6	27.88	1.58
		3	Service	104	0.15	460	30	321.38	465.77	26.6	17.51	
			Ultimate	216	3.00	680	30	657.48	654.40	26.6	24.60	1.40
Average	Service	103.67	0.15	450.00	30	320.35	474.90	26.6	17.85			
Ultimate	217.00	2.00	637.00	30	670.57	704.06	26.6	26.47	1.48			
PP1-Bottom (VF1%)	Bottom	1	Service	119	0.05	470	30	367.73	521.61	26.6	19.61	
			Ultimate	277	2.00	580	30	855.99	983.89	26.6	36.99	1.89
		2	Service	118	0.05	380	30	364.64	639.73	26.6	24.05	
			Ultimate	277	3.00	680	30	855.99	839.20	26.6	31.55	1.31
		3	Service	120	0.05	380	30	370.82	650.57	26.6	24.46	
			Ultimate	275	1.00	580	30	849.81	976.79	26.6	36.72	1.50
Average	Service	119.00	0.05	410.00	30	367.73	603.97	26.6	22.71			
Ultimate	276.33	2.00	613.33	30	853.93	933.29	26.6	35.09	1.55			
PP2-Top (VF2%)	Top	1	Service	103	0.05	460	30	318.29	461.29	23.5	19.63	
			Ultimate	235	1.00	660	30	726.20	733.53	23.5	31.21	1.59
		2	Service	105	0.05	360	30	324.47	600.87	23.5	25.57	
			Ultimate	254	2.00	590	30	784.91	886.90	23.5	37.74	1.48
		3	Service	105	0.05	360	30	324.47	600.87	23.5	25.57	
			Ultimate	253	3.00	580	30	781.82	898.64	23.5	38.24	1.50
Average	Service	104.33	0.05	393.00	30	322.41	554.35	23.5	23.59			
Ultimate	247.33	2.00	610.00	30	764.31	839.69	23.5	35.73	1.51			
PP2-Bottom (VF2%)	Bottom	1	Service	120	0.05	360	30	370.82	686.71	23.5	29.22	
			Ultimate	313	2.00	590	30	967.23	1092.92	23.5	46.51	1.59
		2	Service	120	0.05	380	30	370.82	650.57	23.5	27.68	
			Ultimate	313	3.00	630	30	967.23	1023.53	23.5	43.55	1.57
		3	Service	123	0.05	380	30	380.09	666.83	23.5	28.38	
			Ultimate	312	1.00	600	30	964.14	1071.27	23.5	45.59	1.61
Average	Service	65.00	0.05	373.33	30	373.91	668.04	23.5	28.43			
Ultimate	113.00	2.00	606.67	30	966.20	1062.57	23.5	45.22	1.59			
PP3-Top (VF3%)	Top	1	Service	129	0.05	440	30	398.64	603.99	22.4	26.96	
			Ultimate	257	1.00	560	30	794.18	945.45	22.4	42.21	1.57
		2	Service	129	0.05	460	30	398.64	577.73	22.4	25.79	
			Ultimate	257	2.00	640	30	794.18	827.27	22.4	36.93	1.43
		3	Service	125	0.05	460	30	386.28	559.82	22.4	24.99	
			Ultimate	255	3.00	580	30	788.00	905.75	22.4	40.44	1.62
Average	Service	127.67	0.05	410.00	30	394.52	580.52	22.4	25.92			
Ultimate	256.33	2.00	613.33	30	792.12	892.82	22.4	39.86	1.54			
PP3-Bottom (VF3%)	Bottom	1	Service	147	0.05	460	30	454.26	658.35	22.4	29.39	
			Ultimate	388	2.00	720	30	1199.00	1110.18	22.4	49.56	1.69
		2	Service	147	0.05	380	30	454.26	796.95	22.4	35.58	
			Ultimate	386	3.00	680	30	1192.82	1169.43	22.4	52.21	1.47
		3	Service	150	0.05	480	30	463.53	643.79	22.4	28.74	
			Ultimate	386	1.00	720	30	1192.82	1104.46	22.4	49.31	1.72
Average	Service	148.00	0.05	440.00	30	457.35	699.69	22.4	31.24			
Ultimate	386.67	2.00	706.67	30	1194.88	1128.02	22.4	50.36	1.61			

Notes:

1. Impact Energy = $E = N (m \times g \times h)$
2. Crack Resistance $R = E / (lc \times dc \times wc)$
3. Crack Resistance Ratio, $Cr = R / fcu$
4. Impact Residual Strength Ratio, $Irs = Eu / Es$